AJNR

Direct intracranial sagittal and coronal CT scanning: anatomy and pathology.

R G Bluemm

AJNR Am J Neuroradiol 1983, 4 (3) 484-487
http://www.ajnr.org/content/4/3/484

Direct Intracranial Sagittal and Coronal CT Scanning: Anatomy and Pathology

Rainer G. Bluemm[1]

The application of whole-body scanners with a wide aperture cone to neuroradiology permits examination of the head in the sagittal plane. This method yields better definition of anatomic structures such as the inner and outer supra- and infratentorial cerebrospinal fluid spaces, the major vessels, and all structures of the posterior fossa close to the midline with negligible artifacts. By mono-, bi-, or triplanar approaches, intracranial pathology can be demonstrated exactly with respect to the major anatomic landmarks, without the disadvantages of multiplanar reconstructed views. In combination with an altered positioning for coronal scanning, optimal biplane evaluation of the sellar region is possible. Additional cisternal enhancement studies in variants of empty sella and brainstem tumors may not always be necessary. The sagittal section, like the coronal, can be placed lateral to metallic clips for early detection of tumor recurrence. Limitations are discomfort in positioning and a degradation of image quality caused by metal amalgam fillings.

It has recently been demonstrated [1, 2] that direct (positional) computed tomographic (CT) scanning of the head in the sagittal plane eliminates the well known hypodense artifact within the sella, the hypodense "Hounsfield bars" between the petrous bones, and the hyperdense streaks arising from the internal occipital protuberance. This is due to a more "homogenous" sampling volume. In our practice we have observed a number of situations in which the sagittal and longitudinal sections provide additional and sometimes invaluable information [3–7] with respect to the axial and direct coronal scans. This report summarizes our experience with more than 150 patients, aged 5–75 years, examined by this method to obtain neurologic, neurosurgical, endocrinologic, and maxillofacial surgical information.

Materials and Methods

Our scanner is a Philips Tomoscan 300. This scanner can obtain six to eight 6-mm-thick slices in 78–104 sec, at 8 sec intervals. It has 288 xenon detectors, a primary geometric enlargement field of view of 32 cm diameter, 4 and 8 sec scan times, 600 pulses/scan, 2 msec pulse width, and operates at 120 kVp.

The patient is placed prone, right or left anterior oblique, on an inclined plane at the rear side of the scanner. This keeps the shoulders out of the fan beam. Arms are stretched along the hips, and the right or left cheek lies against a foam plastic head support fixed at the top of the regular examination table. This helps to parallel the longitudinal plane of the head with the scan plane (+ 20° tilt), ensuring that the head accurately follows the automatic table indexing. To eliminate or reduce angulations between the anatomic features and the scan plane it is advisable to use a light pencil in the inner ring of the gantry, a cap on the patient's head labeled with longitudinal strips, and to scan directly the area of interest. Because of the uncomfortable neck position, the duration of the examination should be kept short by using a batch mode procedure. To obtain coronal sections of the sella nearly perpendicular to the sellar floor without greater hyperextension of the neck, the patient's position is modified. The head is turned 90° vertically to the scanning plane, the head holder is replaced by a normal device for coronal scanning, and the body is put in a complete prone position.

For collimations of 6 mm or 3 mm, 300 mA or 428 mA settings were used, respectively. Contrast agents used were megluminamidotrizoate (306 mg/kg) and iopromide (300 mg I/kg of body weight).

Results

The sagittal projection obtained approximates a true sagittal section through the intracranial and facial structures, and is comparable to a longitudinally reconstructed nuclear magnetic resonance (NMR) image. The most interesting anatomy is located in the midline region (fig. 1). The soft tissue above and below the tentorium, in relation to the inner and outer cerebrospinal fluid (CSF) spaces, and in the vicinity of the calvarium and the skull base (including the paranasal sinus), is easily visualized on a 3-mm-thick precontrast midsagittal scan. The scan is tangential to the falx cerebri and the gyri of either side are not clearly seen. The third ventricle, the sylvian aqueduct, and the triangular fourth ventricle are well delineated. The brainstem (composed of the mesencephalon, pons, and the medulla oblongata) is separated from the clivus by the interpeduncular, pontine, and medullary cisterns. The pontomedullary notch is often well visualized. The cisterna cerebellomedullaris separates the inferior vermis from the occipital bone; the superior vermis is well outlined by the vermian cistern. The normal quadrigeminal cistern is perfectly delineated. The major vascular structures of the posterior fossa are easily identified with or without contrast enhancement. The entire length of the basilar artery is seen in the subarachnoid cisterns in front of the brainstem. The

[1] Department of Radiology, Knappschafts-Krankenhaus, University Clinic, In der Schornau 23/25, 4630 Bochum 7, West Germany.

AJNR 4:484–487, May/June 1983 0195-6108/83/0403-0484 $00.00

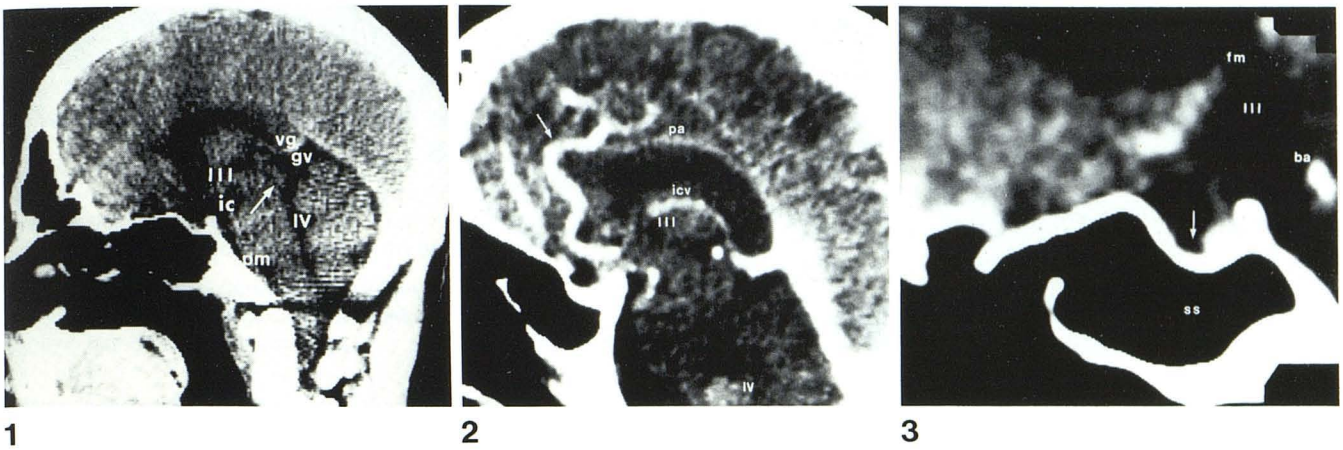

1 2 3

Fig. 1.—3 mm midsagittal section without contrast enhancement in 21-year-old man. Aqueduct (*arrow*). vg = vein of Galen; gv = galenic supravermian cistern; IV = fourth ventricle; pm = pontomedullary cistern; ic = interpeduncular cistern; III = third ventricle.

Fig. 2.—Partly enlarged branches (*arrow*) of postcommunicating anterior cerebral artery leading to frontoparietal angioma (not shown) near convexity. Reduced perfusion of pericallosal artery (pa) (steal effect). icv = intercerebral vein, III = third ventricle; IV = choroid plexus of third and fourth ventricle.

Fig. 3.—Pituitary gland with infundibulum. III = third ventricle; fm = foramen of Monro; ba = basilar artery; ss = sphenoid sinus. CSF in the sella secondary to internal hydrocephalus (*arrow*).

straight sinus and the great vein of Galen form the superior border of the posterior fossa; thus, the free edge of the tentorium is clear.

An angio-CT study of another patient (fig. 2) a few millimeters lateral to the midline demonstrates branches of the postcommunicating anterior cerebral artery and inner cerebral veins. The superior surface is demarcated by the thin callosal artery (steal effect of the enlarged proximal branches, leading to a frontoparietal angioma, not shown in the figure), and parts of the corpus callosum are therefore better visualized. Note also the enhancement of the choroid plexus of the third and fourth ventricles. The gyri of the ipsilateral hemisphere can be better visualized because the falx cerebri is medial to the section.

The relative position or accurate site of intracranial lesions (especially those that are medial or parasagittal with respect to the major external anatomic landmarks) cannot be determined on axial scans alone. The longitudinal view of a 62-year-old patient (fig. 3) indicates where a calvarial meningioma is located with regard to shape, size, and the neighboring brain tissue. There is no substantial loss in density resolution as confirmed by the CT values of the tumor or the gray and white matter. On the axial scans (not illustrated) the tumor could not be defined as clearly, because the sections were tangential to it, and hyperdense streaks of metallic clips of the opposite parietal side (secondary to an earlier operation) degraded the image as well as the coronal slices.

Before the advent of CT in conventional neuroradiology, the lateral plane played an important role in evaluating the sellar region. Sagittal CT offers the additional possibility of delineation with negligible artifacts of the pituitary stalk, which extends from the infundibular recess of the third ventricle inferiorly and slightly anteriorly to reach the pituitary gland (fig. 4). It is also useful in patients lacking obvious sellar enlargement. By means of sagittal sections the curved anterior/posterior walls of the sella can be clearly defined (figs. 4 and 5A). This is not possible with coronal slices. Partial anterior herniation of the diaphragm into a normal-sized sella due to occlusive hydrocephalus can be visualized on a 6-mm-thick section.

It is possible to compare positional scans with reformatted views. Figure 5B illustrates a nearly midsagittal longitudinal view of the same patient as in figure 5A. The view is a computer rearrangement of 13 partly overlapping 5-mm-thick axial sections. A posterior fossa tumor is visible, although the tumor contours appear blurred, and further details of the surrounding structures are difficult to analyze. Figure 5A represents a direct sagittal scan a few millimeters medial to this projection. Apart from the difference in contrast agent kinetics (nearly homogenous enhancement in the direct scan) the image clearly demonstrates the borders of the tumor with respect to the skull base. The longitudinal and vertical dimensions between the tentorium and the foramen magnum are clearly visualized.

The supra-/infratentorial parts of mesencephalic masses can be outlined more precisely than on coronal scans (fig. 6). In this case the cystic tumor compresses the aqueduct and the quadrigeminal cistern but not the interpeduncular and pontine cisterns. The upper part of the fourth ventricle is displaced inferiorly.

Even the so-called half-axial section +25° maximally to the canthomeatal line is limited by interfering metallic dental fillings and degraded by interpetrosal artifacts. In a 43-year-old patient with left-sided central hemiparesis a hypodense lesion secondary to infarction could be clearly defined only in a right parasagittal slice close to the midline (fig. 7).

Discussion

The clinically useful application of direct sagittal CT of the brain extends from the midline to the lateral border of the basal ganglia. Structures described in figures 1–3 can be more easily discriminated and pathologic involvement better delineated in the sagittal projection, according to the principle of sectioning perpendicular to the plane of the object of interest. This also avoids density averaging of rather small soft-tissue structures (e.g., the pituitary gland) with the adjacent bone. The individual combination of scans in the sagittal, coronal, and axial planes allows a mono-, bi-, and triplanar approach to complex lesions—intra-/extraorbital [5, 6]; intra-/suprasellar; intra-/extraventricular; supra-/infratentorial (fig. 6); intra-/extraaxial (fig. 7)—adjacent to the skull base [5, 6], arising from the calvarium or dura, and congenital anomalies [4, 7], even in areas of high attenuation differences [6, 8, 9]. In this way the

Fig. 4.—Accurate location, configuration, and size of calvarial meningioma with respect to adjacent soft tissue and bone in longitudinal plane lateral to metallic clips in 62-year-old patient. Craniotomy was performed due to parietal tumor in opposite side.

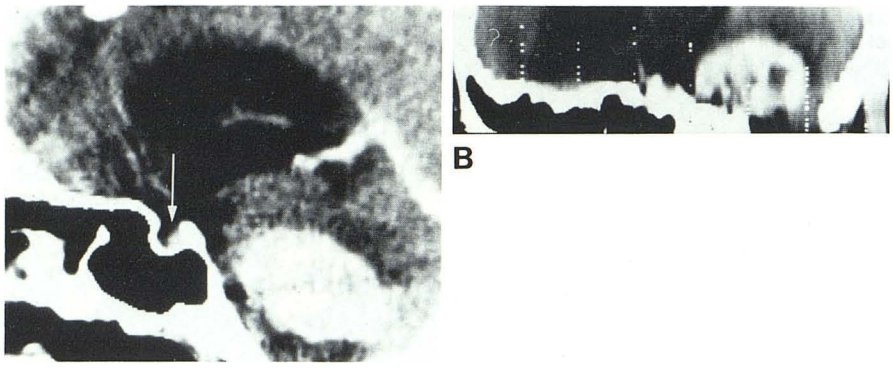

A B

Fig. 5.—Direct sagittal section, 6 mm thick, in 40-year-old patient with progressive loss of hearing and symptoms of increased intracranial pressure. **A**, Exact visualization of tumor size, contours, and relation to neighboring structures. Difference in contrast agent kinetics. Partial anterior herniation of sellar diaphragm (*arrow*) due to occlusive hydrocephalus. **B**, Reformatted longitudinal view of extraaxial posterior fossa tumor, computer-rearranged from 5 mm thick partly overlapping axial slices. Blurred tumor contours. Poorer spatial resolution and inferior topography compared with **A.**

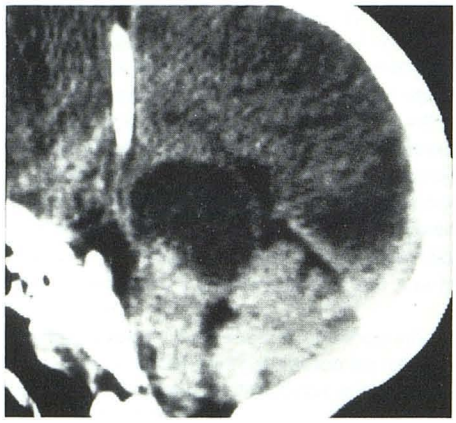

6

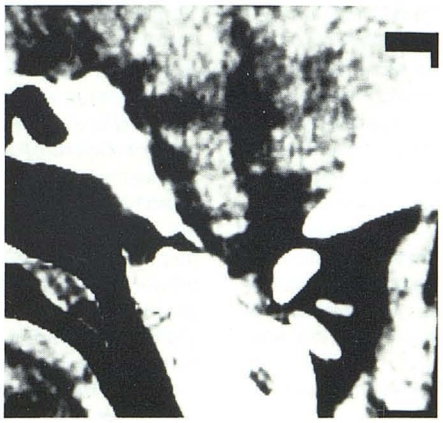

7

Fig. 6.—Cystic mesencephalic tumor. Displacement of roof of fourth ventricle inferiorly. Exact determination of that part of tumor extending below tentorial gap. Interpeduncular and pontine cistern not compressed. Occipital hypodense lesion consistent with secondary ischemic infarction of posterior cerebral artery.

Fig. 7.—Central left hemiparesis in 43-year-old patient. Clearly defined round intraaxial upper brainstem lesion a few millimeters right lateral to midline, secondary to ischemic infarction. This could not be outlined exactly even on axial scans + 25° to baseline (interpetrosal artifact zone). Enlarged cisterns and fourth ventricle due to atrophy.

neurosurgeon or radiotherapist can be provided with *all* necessary information.

As does sagittal CT, coronal scanning of the sellar region as described in this paper produces negligible artifacts, so an optimal biplanar evaluation of all anatomic and pathologic conditions of the sellar area is possible. The diagnostic criteria ruled out by means of different investigational techniques [1, 10–13] can be easily applied. In our opinion, variants of an empty sella do not necessarily require an additional metrizamide or air study. Situations and complications before and after transsphenoidal surgery can be easily determined on sagittal sections [4, 6, 7] as far as the operative route, the filling material after tumor removal, and leakage of CSF or air are concerned.

Except for NMR, sagittal CT is the only technique by which interpetrosal artifacts do not occur. To date, different approaches to this problem have failed to offer a definite solution [12, 14]. This underscores its value for the assessment of lesions related to the brainstem (e.g., pontomedullary and extrinsic brainstem tumors arising from the clivus). As it facilitates the definition of tumors of the entire posterior fossa in combination with selected axial and coronal sections, it may be an alternative to cisternal metrizamide-enhanced studies [15].

The detection of cerebellar and brainstem atrophy is notably improved by midsagittal slices (fig. 7) [16, 17], but, to explore the entire posterior fossa sagittal reconstruction, at least 24 and often 34 overlapping 5-mm-thick axial scans have to be obtained [18]. The sylvian aqueduct and the third ventricle are normally not seen on these computer-rearranged views [18]. To apply 1.5 mm overlapping axial slices does not seem routinely practicable. Linear interpolation [2] (greater image size than display matrix pixel area) accounts for the coarse and blurred structure contours (fig. 5B). For this reason and the stripelike view, topography is less easily delineated than on a direct section with complete information. Therefore, whenever possible, a lesion should be examined directly.

Tumors and malformations in the midline predominate in infantile intracranial pathology [11]. Sagittal scans are easily obtained in children, since the motility of their cervical spine is normal. The results are excellent with regard to tumor stagings and definition of primary and secondary lesions in the region of the aqueduct. The understanding of complex malformations and their rudimentary variants is better [7]. Also, the radiation dose received by the lenses of the eye during sagittal scanning is significantly lower in the midline region [19]. This has been confirmed by our own thermoluminescent dosimetric data.

Like the coronal section, sagittal CT may be especially helpful if set lateral to metallic clips, so that streaks degrading the image may be avoided. This can be very important for early detection of tumor recurrence.

But sagittal CT has its limitations. Difficulty is experienced with large or obese patients and those who have inflexible cervical spines because of preexisting degenerative pathology. Also, amalgam fillings and other metallic tooth implantations may cause streak artifacts that detract from the image quality. Fortunately, the incisions usually have fewer implants than the molars.

Editor's Note: Structures demonstrated here by direct sagittal section are also often visualized by multiplanar reconstructed images on high-resolution instruments.

REFERENCES

1. Bluemm RG. Direkte sagittale Computertomographie des Hirnschaedels. Methodik und erste Ergebnisse. *Dtsch Med Wochenschr* **1981**;106:1416–1417
2. Bluemm RG. Direct sagittal (positional) computed tomography of the head. *Neuroradiology* **1982**;22:199–201
3. Bluemm RG. Direct sagittal computed tomography of the head. Presented at the 6th Carvat international meeting on body CT and new imaging, Rome, February **1982**
4. Bluemm RG. Ergebnisse der sagittalen Computertomographie des Schaedels. Scientific exhibit. Presented at the annual meeting of the German Radiological Society, Berlin, May **1982**
5. Bluemm RG, Akuamoa-Boateng E, Dieckmann J. Direkte sagittale Computertomographie des Gesichtsschaedels. Methodik und erst klinische Ergebnisse. Presented at the annual meeting of the German Society of Oral and Maxillo-Facial Surgery, Luebeck-Travemuende, May **1982**
6. Bluemm RG, van Waes PFGM. Direct sagittal computed tomography of the base of the skull. Presented at the 9th International Congress of Radiology in Otolaryngology, Fontevraud, France, June **1982**
7. Bluemm RG. Direct sagittal computed tomography in children. Presented at the 8th meeting of the European Society of Pediatric Surgery, Rennes, France, June **1982**
8. Mass S, Norman D, Newton TH. Coronal computed tomography: indications and accuracy. *AJR* **1978**;131:875–879
9. Nakagawa H, Wolf BS. Delineation of lesions of the base of the skull by computed tomography. *Radiology* **1977**;124:75–80
10. Aubin ML, Bentson J, Vignaud J. Tomodensitométrie de la tige pituitaire. *J Neuroradiol* **1978**;5:153–160
11. Clar HE, Bock JW, Weichert HC. Comparison of encephalotomograms and computerized tomograms in midline tumors in infants. *Acta Neurochir* (Wien) **1979**;50:91–101
12. Earnest NF, McCullough EC, Frank DA. Fact or artifact: an analysis of artifact in high-resolution computed tomographic scanning of the sella. *Radiology* **1981**;140:109–113
13. Syvertsen A, Haughton VM, Williams AL, Cusick JF. The computed tomographic appearance of the normal pituitary gland and pituitary microadenomas. *Radiology* **1979**;133:385–391
14. Glover GH, Pelc NJ. Nonlinear partial-volume artifacts in x-ray computed tomography. *Med Phys* **1980**;7:238–248
15. Glanz S, Geehr RB, Duncan CC, Piepmeier JM. Metrizamide-enhanced CT for evaluation of brainstem tumors. *AJNR* **1980**;1:31–34;*AJR* **1980**;134:821–824
16. Baker HL. The clinical usefulness of routine coronal and sagittal reconstructions in cranial computed tomography. *Radiology* **1981**;140:1–9
17. Bluemm RG, Gehlen W. Aspects of direct (positional) sagittal CT-scanning of the brain with respect to clinical findings. *Acta Neurochi* (Wien) **1982**;66:213–220
18. Delavelle J, Megret M. CT sagittal reconstruction of posterior fossa tumors. *Neuroradiology* **1980**;19:81–88
19. Kronholz HL, Castrup W, Glasmeier KH. Zur Strahlenbelastung von Kindern bei Schaedeluntersuchungen an Computertomographen der neuen Generation. Presented at the annual meeting of the German Radiological Society, Munich, May **1981**